Geoderma 461 (2025) 117486

Contents lists available at ScienceDirect

Geoderma

journal homepage: www.elsevier.com/locate/geoderma

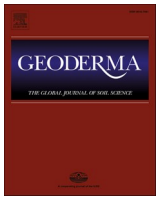

Heavy metal contamination threats carbon sequestration of paddy soils with an attenuated microbial anabolism

Li Xiong [a,b,c,d], Marios Drosos [e], Min Jiao [f], Jianfei Sun [g], Guilong Li [a,b], Longxin He [a,b], Fan Li [a,b], Cheng Liu [h], Antonio Scopa [e], Wenjian Xia [a,b,*], Caihong Shao [a,b], Zengbing Liu [a,b]

[a] Institute of Soil and Fertilizer & Resources and Environment, Jiangxi Academy of Agricultural Sciences, Nanchang 330200, China
[b] National Engineering and Technology Research Center for Red Soil Improvement, Nanchang 330200, China
[c] Key Laboratory of Crop Ecophysiology and Farming System for the Middle and Lower Reaches of the Yangtze River, Ministry of Agriculture and Rural Affairs, Nanchang 330200, China
[d] Jiangxi Provincial Key Laboratory of Arable Land Improvement and Quality Enhancement, Nanchang 330200, China
[e] Department of Agricultural, Forest, Food, and Environmental Sciences, University of Basilicata, Viale Dell'Ateneo Lucano 10, 85100 Potenza, Italy
[f] Agricultural Technology Extension Center of Jiangxi Province, Nanchang 330046, China
[g] Nanjing Institute of Environmental Sciences, Ministry of Ecology and Environment of the People's Republic of China, Nanjing 210042, China
[h] School of Environment and Natural Resources, Zhejiang University of Science and Technology, Hangzhou 310023, China

ARTICLE INFO

Handling Editor: Dr Cornelia Rumpel

Keywords:
Soil organic carbon
Microbial carbon use efficiency
Microbial residues
Heavy metal pollution
Rice paddies

ABSTRACT

As a global environmental concern, heavy metal pollution significantly impacts soil organic carbon (SOC) dynamics. Nevertheless, the microbial mechanisms governing SOC persistence under heavy metal contamination remain unclear, as previous research primarily focused on microbial catabolism. This study elucidated SOC variation induced by heavy metal contamination from the perspective of microbial anabolism, a key contributor to SOC sequestration according to recent theory. Herein a field survey was conducted at 13 sampling sites in polluted rice paddies, determining both SOC content and key microbial parameters. Nemerow index (a comprehensive index of pollution level) ranged from 0.48 to 2.93, with cadmium and copper as the primary contaminants. SOC content ranged between 14.56 and 23.97g kg^{-1} across sampling sites and showed a negative relationship with nemerow index ($R^2 = 0.46, P < 0.001$). Variation partitioning and random forest analyses indicated that SOC reduction was primarily driven by the combined effects of microbial factors and heavy metal pollution, with dominant role of microbial factors. Nemerow index negatively correlated with microbial C use efficiency (CUE) ($R^2 = 0.42, P < 0.001$) and microbial biomass turnover ($R^2 = 0.12, P = 0.017$). Structural equation modeling further suggested that heavy metal pollution reduced SOC by decreasing microbial biomass carbon (MBC) formation and microbial residue accumulation through negative effects on microbial CUE and soil nitrogen availability. Collectively, our research provided robust evidences that heavy metal pollution could threat C sequestration of paddy soils by attenuating microbial anabolism with reduced accumulation of microbial-derived carbon.

1. Introduction

Soil organic carbon (SOC) in croplands is not only the foundation of soil fertility and productivity (Lal, 2004), but also plays a significant role in mitigating climate change by accounting for almost 10 % of the global SOC pool in the top 1 m of soil cover (Batjes, 1996; Jobbágy and Jackson, 2000). The ecological functions of SOC largely depend on its cycling, transformation, and persistence, and these processes are profoundly affected by environmental stressors like heavy metal pollution (Bian et al., 2015; Zeng et al., 2024a). With intensive anthropogenic activities over the past century, heavy metal contamination of cropland soils is growing into a global issue with severely toxic effects on soil quality/health and food security (Khan et al., 2021; Qin et al., 2021). As primary regulator of soil C cycling, microorganisms act as "the eye of the needle" through which SOC can be mediated (Paterson et al., 2009) and are highly sensitive to heavy metals (Abdu et al., 2017). Consequently, the influences of heavy metal pollution on microbially mediated SOC transformation are attracting increasing attention (Xiao et al., 2023;

* Corresponding author at: Jiangxi Academy of Agricultural Sciences, Nanchang 330200, China.
E-mail address: xiawenjian@163.com (W. Xia).

https://doi.org/10.1016/j.geoderma.2025.117486
Received 17 April 2025; Received in revised form 16 July 2025; Accepted 19 August 2025
Available online 23 August 2025

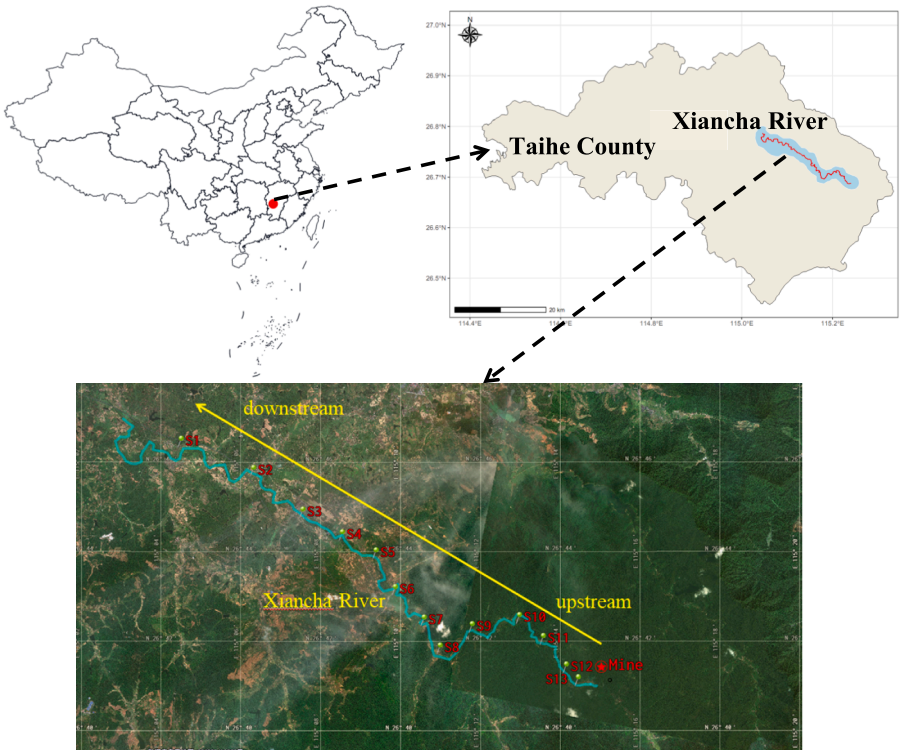

Fig. 1. Location of the study area and the 13 sampling sites along the Xiancha River.

Table 1
Heavy metal content and nemerow index in the different sampling sites.

Sampling site	Total Cd content (mg kg^{-1})	Total Cu content (mg kg^{-1})	Nemerow index	Distance to the mine (km)
S1	0.17 ± 0.02f	29.68 ± 1.55e	0.48 ± 0.04f	17.5
S2	0.38 ± 0.02e	55.65 ± 3.20d	0.96 ± 0.13e	14.2
S3	0.46 ± 0.03de	65.64 ± 3.30d	1.14 ± 0.06de	12.7
S4	0.60 ± 0.02 cd	65.35 ± 2.34d	1.48 ± 0.12 cd	11.0
S5	0.57 ± 0.04 cd	72.26 ± 3.38d	1.42 ± 0.14 cd	9.4
S6	0.63 ± 0.06c	108.74 ± 3.06c	1.62 ± 0.24c	8.5
S7	0.54 ± 0.04 cd	71.84 ± 5.40d	1.37 ± 0.16cde	7.5
S8	0.63 ± 0.02c	110.30 ± 7.44c	1.64 ± 0.10c	6.7
S9	0.91 ± 0.05b	119.72 ± 5.08c	2.23 ± 0.16b	5.4
S10	0.93 ± 0.04b	153.85 ± 6.43b	2.29 ± 0.12b	3.4
S11	1.20 ± 0.05a	181.68 ± 11.15a	2.93 ± 0.16a	2.4
S12	1.01 ± 0.10b	193.33 ± 10.94a	2.86 ± 0.17a	1.6
S13	0.91 ± 0.09b	190.52 ± 18.25a	2.78 ± 0.23a	0.9

The risk screening values are 0.3 mg kg^{-1} and 50 mg kg^{-1} for Cd and Cu, respectively. Different lowercase letters in a single column indicate significant difference among the sampling sites (Tukey's HSD test, $P < 0.05$).

Zeng et al., 2024b).

Microorganisms execute two contrasting but critical roles in determining soil C dynamics: reducing SOC accumulation via microbial catabolism with CO_2 release, and promoting SOC accrual via anabolic processes with formation of microbial biomass and microbial residues (Liang et al., 2017; Tao et al., 2023). Numerous studies have confirmed that heavy metal pollution could significantly alter microbial activity, diversity, and their community composition (Dai et al., 2004; Enya et al., 2020; Ohm et al., 2011). However, most previous research merely focused on the effects of these altered microbial properties on catabolic processes with various results including suppressed or enhanced microbial respiration (Dai et al., 2004; Wang et al., 2022). Recent studies highlight the substantial contribution of microbial anabolism to SOC sequestration in cropland soils (more than 50 %), driven by the continuous production of microbial residues during the iterative processes of cell growth, proliferation, and death (Chen et al., 2021; Liang et al., 2017). Furthermore, microbial residues can be preferentially stabilized through association with soil minerals (Xiao et al., 2023), establishing them as the key components of the stable SOC pool with persistence timescales ranging from decades to millennia (Cotrufo et al., 2013; Georgiou et al., 2017). Despite this understanding, the direction and magnitude of heavy metal-induced changes in microbial properties on anabolic processes remain unclear. This knowledge gap impedes a comprehensive assessment of SOC transformation and persistence in contaminated soils, particularly given the essential role of microbial anabolism in SOC dynamics.

To our knowledge, only two studies reported the variation of microbial residues under heavy metal contamination. Kandeler et al. (2000) found that heavy metal pollution reduced amino sugar content (a biomarker of microbial residues) by 25.09 % in a dryland farming system. Liu et al. (2023) further reported a decreased contribution of microbial residues to SOC in apple orchards under heavy metal pollution. Although these results implied that heavy metal pollution may decrease SOC storage by reducing the accumulation of microbial residues through impaired microbial anabolism, further investigations should be conducted in different agricultural systems. Moreover, the inherent mechanisms of above clue remain unresolved, creating a huge knowledge gap in understanding the SOC persistence mediated by microbial anabolism under heavy metal pollution. Microbial physiological traits, microbial C

Table 2
Soil physicochemical properties in the different sampling sites.

Sampling site	pH value	SOC content (g kg^{-1})	TN content (g kg^{-1})	TP content (g kg^{-1})	TK content (g kg^{-1})	HN content (mg kg^{-1})	AP content (mg kg^{-1})	AK content (mg kg^{-1})	CEC value ($cmol_{(+)}$ kg^{-1})	Clay content (%)
S1	4.83 ± 0.07 f	21.99 ± 1.93 ab	2.27 ± 0.17 cd	0.76 ± 0.07 c	18.29 ± 3.01 a	153.36 ± 13.52 bcd	38.94 ± 2.82 c	93.73 ± 7.13 e	6.10 ± 1.01 f	15.02 ± 1.76 bc
S2	5.26 ± 0.05 bc	22.70 ± 2.55 ab	2.76 ± 0.27 a	0.98 ± 0.17 abc	18.54 ± 1.01 a	190.51 ± 17.89 abc	50.77 ± 6.50 abc	95.14 ± 3.73 e	10.82 ± 0.70 bc	16.29 ± 1.46 ab
S3	4.79 ± 0.06 f	20.79 ± 2.31 abc	2.80 ± 0.02 a	1.01 ± 0.08 abc	21.90 ± 2.49 a	190.17 ± 20.15 abc	45.40 ± 5.16 bc	166.32 ± 15.31 bcd	10.24 ± 0.89 c	20.02 ± 1.50 a
S4	5.86 ± 0.08 a	20.88 ± 1.67 abc	2.71 ± 0.05 ab	1.05 ± 0.07 ab	22.41 ± 2.09 a	195.36 ± 17.66 ab	66.37 ± 4.90 a	204.20 ± 16.72 ab	10.13 ± 0.27 c	15.55 ± 1.77 bc
S5	5.01 ± 0.12 def	22.75 ± 1.46 ab	2.42 ± 0.11 abc	0.89 ± 0.09 abc	20.67 ± 3.38 a	227.41 ± 23.15 a	48.84 ± 7.93 bc	159.46 ± 20.04 cd	9.37 ± 1.20 cde	14.44 ± 1.38 bc
S6	5.42 ± 0.13 b	23.97 ± 1.82 a	2.52 ± 0.05 abc	0.83 ± 0.09 bc	21.28 ± 2.47 a	186.90 ± 14.51 abc	40.51 ± 4.14 c	128.54 ± 10.51 de	13.28 ± 0.82 a	15.09 ± 1.09 bc
S7	5.34 ± 0.08 bc	19.42 ± 1.69 abcd	1.90 ± 0.28 def	0.99 ± 0.09 abc	23.44 ± 2.32 a	134.10 ± 12.57 de	58.78 ± 6.39 ab	225.21 ± 16.95 a	9.72 ± 0.72 cde	15.30 ± 0.90 bc
S8	5.22 ± 0.03 bcd	18.61 ± 2.01 abcd	2.33 ± 0.08 bc	0.83 ± 0.08 bc	24.03 ± 1.75 a	186.92 ± 17.54 abc	44.51 ± 4.47 bc	136.24 ± 11.27 d	12.95 ± 1.15 ab	14.75 ± 0.89 bc
S9	5.14 ± 0.02 cde	15.27 ± 2.46 cd	1.54 ± 0.09 fg	1.03 ± 0.11 abc	21.65 ± 2.85 a	97.44 ± 7.80 e	57.13 ± 4.98 ab	162.85 ± 11.86 cd	7.59 ± 0.72 def	14.77 ± 1.47 bc
S10	5.21 ± 0.04bcd	14.64 ± 1.75 d	1.80 ± 0.06 ef	0.76 ± 0.06 c	19.73 ± 1.54 a	134.09 ± 14.11 de	45.03 ± 3.55 bc	93.98 ± 6.65 e	7.48 ± 0.55 def	14.54 ± 0.74 bc
S11	4.96 ± 0.11 ef	17.27 ± 1.17 bcd	2.17 ± 0.12 cde	0.89 ± 0.11 abc	19.33 ± 3.01 a	144.21 ± 13.68 cde	51.79 ± 4.91 abc	164.65 ± 16.88 bcd	9.77 ± 0.67 cd	14.01 ± 1.36 bc
S12	5.23 ± 0.11 bcd	16.90 ± 1.57 bcd	1.21 ± 0.04 g	1.02 ± 0.09 abc	18.00 ± 1.79 a	153.68 ± 12.50 bcd	45.38 ± 5.00 bc	159.26 ± 15.09 cd	7.30 ± 0.78 ef	15.20 ± 1.69 bc
S13	5.35 ± 0.06 bc	14.56 ± 3.10 d	1.86 ± 0.12 ef	1.16 ± 0.07 a	21.71 ± 1.68 a	125.48 ± 14.02 de	66.47 ± 6.65 a	177.37 ± 13.18 bc	6.77 ± 0.84 f	11.75 ± 1.25 c

Different lowercase letters in a single column indicate significant difference among the sampling sites (Tukey's HSD test, $P < 0.05$).

use efficiency (CUE) and microbial biomass turnover, are critical parameters to regulate microbial residue accumulation (Tao et al., 2023; Wang et al., 2021). Microbial CUE, defined as the ratio of microbial assimilation of C for growth to the total C uptake, integrates microbial metabolic processes governing SOC cycling (He et al., 2023; Spohn et al., 2016). A low CUE indicates that more carbon is used for respiration relative to biosynthesis in microbial metabolism; whereas high CUE generally means a promoted biomass synthesis and residue formation (Manzoni et al., 2012). Previous studies suggested that heavy metal pollution could decrease microbial CUE (Wang et al., 2022; Xu et al., 2018), implying impaired anabolic processes with less microbial residue production. On the other hand, heavy metal stress may accelerate microbial biomass turnover considering toxic living condition, which could lead to a fast production rate of microbial residues (Spohn et al., 2016). Therefore, how heavy metal pollution affects the accumulation of microbial residues via their physiological traits remains equivocal and lacks empirical validation.

As distinctive anthropogenic soils (Anthrosols), paddy soils exhibit an enormous capacity of C sequestration with storage of 18 Pg C in the depth of 1 m, accounting for 14 % of SOC pool in croplands (Liu et al., 2021). China possesses the world's largest rice cultivation area (over 30 million hectares), with approximately half distributed in southern China (Wei et al., 2022), a major nonferrous mining region. Consequently, massive heavy metals were released into environment through wastewater and dust during mining and smelting activities, causing severe paddy soil contamination (Jiang et al., 2021; Lin et al., 2019). Therefore, a field survey was conducted in paddy fields at an abandoned tungsten mine in order to reveal how heavy metal pollution affects SOC dynamics through microbial anabolic processes. To achieve this purpose, the relationships among heavy metal pollution, microbial physiological traits, microbial biomass and microbial residues, soil physicochemical properties, and SOC content were quantified. We hypothesized that (1) heavy metal contamination will decrease microbial CUE and accelerate microbial biomass turnover; (2) attenuated microbial anabolism will be found and will contribute substantially to SOC variation in polluted paddy soils. This study may greatly advance our knowledge of SOC transformation and sequestration driven by microbial process in paddy fields with heavy metal pollution.

2. Materials and methods

2.1. Site description and soil sampling

Field research was conducted in the vicinity of Xiaolong tungsten mine, which was exploited since 1934 and closed in 2020. The mine is located at Xiaolong town in Taihe county of Jiangxi Province, China (26°41′26″ N, 115°15′5″ E) (Fig. 1), and the area is prevailed by subtropical monsoon climate with mean annual temperature of 18.6 ℃ and mean annual precipitation of 1726 mm. Rice paddies are the most important type of agricultural lands in this region with a typical early rice-late rice rotation system. As recommended by the local agricultural technology extension center, paddy fields received 150 kg N, 80 kg

Table 3
Soil microbial properties in the different sampling sites.

Sampling site	Amino sugar content (mg kg^{-1})	MBC content (mg kg^{-1})	Microbial CUE	Microbial turnover time (day)
S1	1519.65 ± 72.50b	678.23 ± 67.32bc	0.32 ± 0.04ab	93.65 ± 9.43ab
S2	1740.34 ± 105.34a	847.70 ± 18.19a	0.39 ± 0.04a	84.52 ± 14.29abc
S3	1475.67 ± 42.77bc	795.35 ± 27.29ab	0.37 ± 0.03a	90.07 ± 13.18abc
S4	1500.88 ± 41.95b	769.65 ± 68.29ab	0.36 ± 0.05a	105.30 ± 12.61a
S5	1298.49 ± 30.65d	690.86 ± 31.40bc	0.40 ± 0.06a	65.57 ± 11.38cde
S6	1388.88 ± 44.98bcd	567.46 ± 47.91c	0.40 ± 0.05a	35.90 ± 2.62f
S7	1315.68 ± 85.25 cd	228.55 ± 28.32f	0.41 ± 0.04a	85.18 ± 8.16abc
S8	1346.00 ± 67.03bcd	435.53 ± 27.00d	0.42 ± 0.05a	76.48 ± 9.30bcd
S9	985.36 ± 45.03ef	381.27 ± 53.99de	0.15 ± 0.06 cd	99.05 ± 5.88ab
S10	1096.44 ± 32.23e	389.76 ± 25.49de	0.20 ± 0.06bcd	92.54 ± 9.31abc
S11	1111.04 ± 76.09e	343.48 ± 37.91def	0.21 ± 0.04bcd	49.19 ± 7.59def
S12	881.42 ± 26.22f	359.84 ± 37.09de	0.28 ± 0.03abc	79.94 ± 3.90abc
S13	701.48 ± 30.10 g	268.62 ± 42.99ef	0.14 ± 0.04d	41.58 ± 7.31ef

Different lowercase letters in a single column indicate significant difference among the sampling sites (Tukey's HSD test, $P < 0.05$).

P_2O_5, and 150 kg K_2O per hectare during early rice season, and 180 kg N, 80 kg P_2O_5, and 150 kg K_2O during late rice season. This fertilization regimen was widely adopted by farmers for over a decade. Following local practice, P_2O_5 and K_2O were applied as compound fertilizer (N: P_2O_5: K_2O = 15: 15: 15), N was applied as urea (46 % N) and compound fertilizer. As the water resource for rice cultivation, the Xiancha River flows through the study area. Previous study indicated that paddy fields in Xiancha River basin were contaminated by heavy metals due to irrigation with polluted river water with more than 80 years of mining activities (Guo et al., 2022).

Soil samples were collected from 13 sites along the river from upstream to downstream after rice harvesting in October 2022 (Fig. 1), and three adjacent paddy fields were selected as triplicates in each site. In each field, five 2 × 2 m plots were established, and five random soil cores (2.5 cm in diameter) from surface layer (0–20 cm) were taken in each sampling plot. Cores from all plots within a field were homogenized into a composite sample. Samples were shipped to the lab within 24 h and sieved through a 2-mm sieve to remove plant roots, stones, and debris. Each fresh sample was divided into two parts, the first part stored at 4 ℃ for microbial physiological trait analysis, and the other part air-dried at room temperature for analyzing soil pH, hydrolyzed nitrogen (HN), available phosphorus (AP), available potassium (AK), cation exchange capacity (CEC), and clay content. Moreover, the air-dried soil samples were ground to pass through a 0.15-mm sieve for analysis of heavy metals, SOC, total nitrogen (TN), total phosphorus (TP), total potassium (TK), and amino sugars.

2.2. Analysis of microbial physiological traits

Microbial CUE and microbial biomass turnover were determined via the ^{18}O-H_2O tracer approach (Spohn et al., 2016). Firstly, soil samples were pre-incubated at 25 ℃ for 7 days with 60 % water holding capacity. Duplicate aliquots of pre-incubated soil (0.6 g) were transferred to vials (2 ml). To achieve 20.0 atom% ^{18}O-labeled soil water, one replicate received ^{18}O-H_2O (97.0 atom% ^{18}O), while the control received an equivalent volume of deionized water. Vials were transferred to headspace bottles (20 ml), capped, and then flushed with CO_2-free air for 5 min. Three soil-free bottles served as CO_2 blanks. All the bottles were incubated at 25 ℃ for 24 h. After incubation, gas samples were taken from the bottles via syringe for CO_2 quantification with a gas chromatograph (Agilent 7890B, Agilent Technologies). Soil DNA was extracted with a DNA extraction kit (MoBio, Powersoil) according to the manufacturer's procedures, and quantified by PicoGreen assay (Quant-iT™ PicoGreen dsDNA Reagent, Life Technologies) with microplate spectrophotometer (Multiskan SkyHigh, Thermo Fisher - Scientific). Subsequently, 50 μl of DNA extracts were dried in a silver capsule at 60 ℃ for 8h. O content and ^{18}O abundance were measured by a thermochemical elemental analyzer coupled with isotope ratio mass spectrometer (TC/EA-IRMS, Thermo Fisher). The $CHCl_3$ fumigation extraction method was used to determine soil microbial biomass C (MBC) content with extraction efficiency of 0.45 (Wu et al., 1990).

As depicted by Spohn et al. (2016), total dsDNA produced ($DNA_{produced}$) during incubation period (24 h) was calculated by equation (1):

$$DNA_{produced}(\mu g) = O_{content} \times \frac{at\%_{excess}}{100} \times \frac{100}{at\%_{final}} \times \frac{100}{31.21} \quad (1)$$

where $O_{content}$ is total O content (μg) of the dried DNA extracts; $at\%_{excess}$ is atom% ^{18}O of the labeled sample subtracted by atom% ^{18}O of the non-labeled sample; $at\%_{final}$ is the obtained atom% ^{18}O of soil–water (20.0 % in our study); the constant of 31.21 represents the average weight percentage of O in DNA.

Conversion factor (f_{DNA}) was calculated with the ratio of MBC to DNA content for each soil sample, and was then applied to compute the microbial growth rate (M_{growth}) by equation (2):

$$M_{growth}(\text{ng C g}^{-1}\text{ soil h}^{-1}) = \frac{f_{DNA} \times DNA_{produced} \times 1000}{DW \times t} \quad (2)$$

where DW (g) is dry weight of soil and t (h) is incubation time.

Microbial respiration rate ($M_{respiration}$) was calculated by equation (3):

$$M_{respiration}(\text{ng C g}^{-1}\text{ soil h}^{-1}) = \frac{R_s}{DW \times t} \times \frac{p \times n}{R \times T} \times V \times 1000 \quad (3)$$

where R_s (ppm) is CO_2 amount produced during incubation period; p (kPa) is the atmospheric pressure; n (12.01 g mol^{-1}) is the molecular mass of C element; R (8.314 J mol^{-1} K^{-1}) is the ideal gas constant; T (295.15 K) is the absolute temperature of gas; and V (L) is the headspace vial volume.

Finally, microbial CUE and microbial turnover time were respectively calculated by equations (4) and (5):

$$CUE = \frac{M_{growth}}{M_{growth} + M_{respiration}} \quad (4)$$

$$Microbial\ turnover\ time(\text{day}) = \frac{MBC \times 1000}{M_{growth} \times 24} \quad (5)$$

2.3. Amino sugar measurement

The analysis method of amino sugars mainly referred to Zhang and Amelung (1996). Briefly, each soil sample (containing ≥ 0.3 mg N) was hydrolyzed using 6 M HCl (10 ml) at 105 ℃ for 8 h. The hydrolysate was mixed with 100 μl of myo-inositol (internal standard) and then filtered. The solution was adjusted to pH 6.6–6.8 using 1 M KOH and 0.01 M HCl, and dried by rotary evaporation after centrifugation (3000 g for 10 min). The obtained residues were transferred to a vial (3 ml) with methanol (5 ml) and dried by N_2. After that, the residues were re-dissolved by deionized water (1 ml), mixed with 100 μl of N-methylglucamine (quantitative standard), and freeze-dried. The derivatization reagent was prepared by dissolving 32 mg ml^{-1} of hydroxylamine hydrochloride and 40 mg ml^{-1} of 4-(dimethylamino)pyridine in a pyridine-methanol

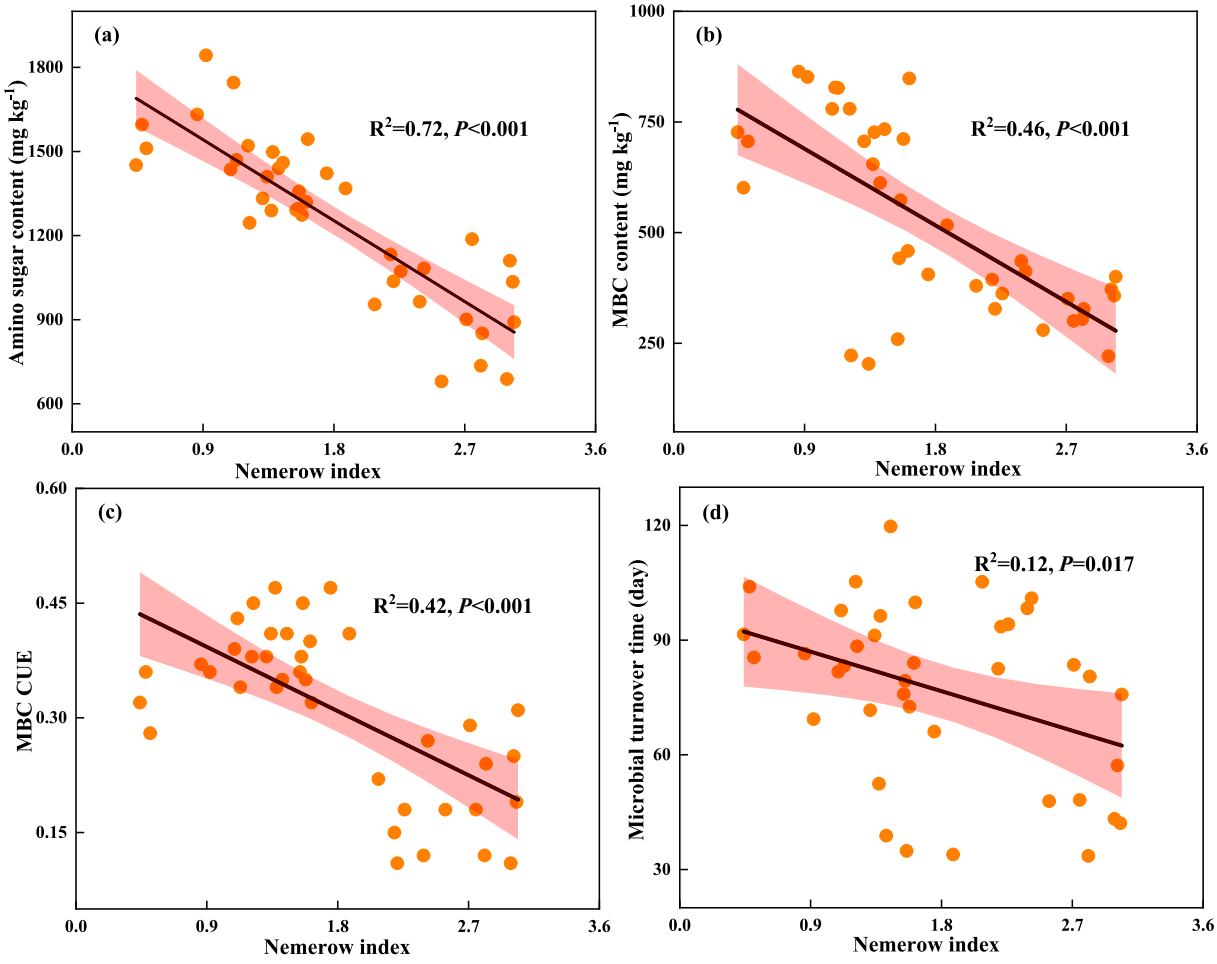

Fig. 2. Relationship between nemerow index and microbial variables: (a) amino sugar content, (b) MBC content, (c) microbial CUE, (d) microbial turnover time.

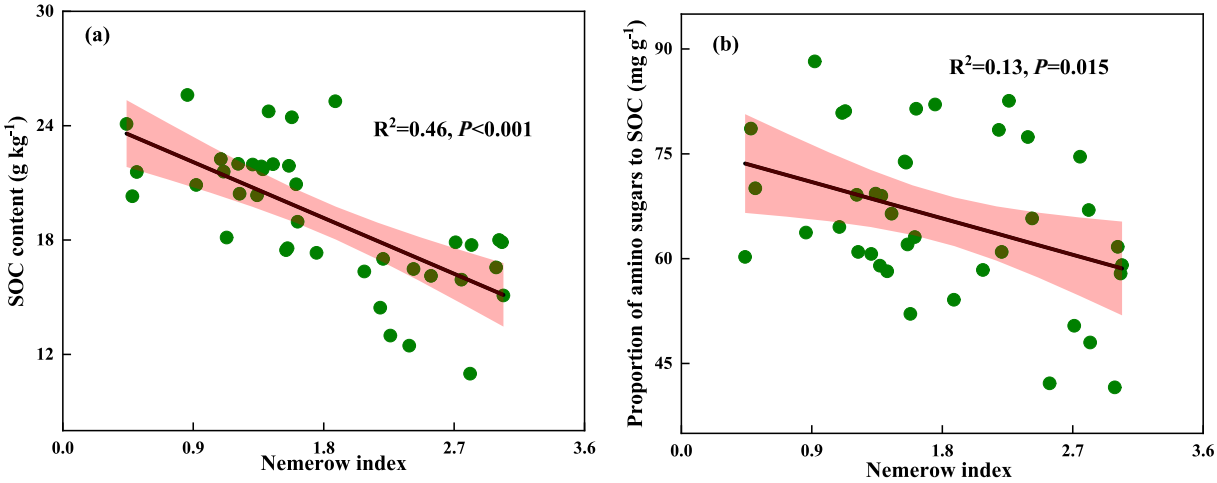

Fig. 3. Relationship of nemerow index with (a) SOC content and (b) proportion of amino sugars in SOC.

mixture (4/1, v/v). The aldononitrile derivatives were then prepared by dissolving the lyophilized residues in 300 μl of the derivatization reagent and heating in a water bath at 75–80 °C for 35 min. After cooling, the solution was mixed with 1 ml of acetic anhydride and heated at 75–80 °C for 25 min. Again after cooling, it was blended with 1.5 ml of dichloromethane and 1 ml of 1 M HCl, and then vortexed at 25 °C for 30 s. The excess derivatization reagents were extracted with 1 ml of deionized water, and then the amino sugar derivatives were dried with N_2 and dissolved in 300 μl of a hexane–ethyl acetate mixture (1/1, v/v) for quantification. Amino sugars were measured by a gas chromatograph equipped with a flame ionization detector (Agilent 7890B GC, Agilent Technologies) and an HP-5 fused silica column (30 m × 0.25 mm × 0.25 μm). Total microbial residues were calculated as the sum of muramic acid, galactosamine, glucosamine, and mannosamine. The determination of amino sugars and microbial physiological traits was performed by Baihui Biotechnology Co. Ltd., at Chengdu, China.

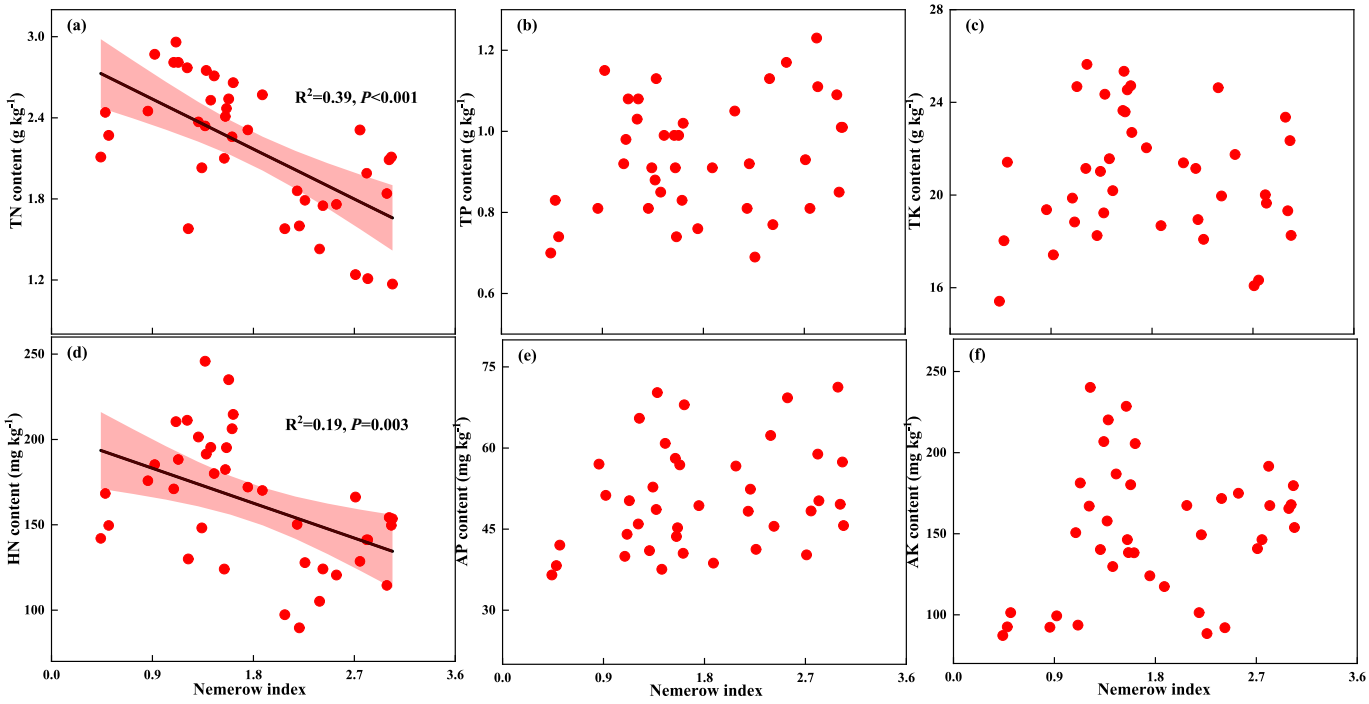

Fig. 4. Relationship between nemerow index and soil nutrients: (a) TN content, (b) TP content, (c) TK content, (d) HN content, (e) AP content, (f) AK content.

2.4. Soil properties detection

As described by Lu (2000), soil samples were digested with HF-$HClO_4$-HNO_3 (8/2.5/2.5, v/v/v) and analyzed for cadmium (Cd), copper (Cu), chromium (Cr), nickel (Ni), lead (Pb), and zinc (Zn) using inductively coupled plasma mass spectrometry (ICP-MS) (aurora M90, Bruker Daltonics). For arsenic (As) and mercury (Hg), digestion was performed with HCl-HNO_3 (1/1, v/v), followed by atomic fluorescence spectrophotometer measurement (AF-610, Bejing Ruili Instruments). The nemerow index (P_N) was adopted to evaluate pollution levels at each sampling site (Tomczyk et al., 2023), calculated using equations (6) and (7):

$$P_i = \frac{C_i}{S_i} \tag{6}$$

$$P_N = \sqrt{\frac{(P_{iave})^2 + (P_{imax})^2}{2}} \tag{7}$$

where P_i is the single pollution index of heavy metal i (eight P_i values per site in our study); C_i is the measured concentration (mg kg^{-1}) of heavy metal i; S_i is the screening value (mg kg^{-1}) of heavy metal i according to the soil environmental quality standard of Chinese agricultural land (GB 15618–2018). P_{iave} is the average value of the eight P_i values in each site, P_{imax} is the maximum value among the eight P_i indices per site. The evaluation and classification of heavy metal contamination was shown in Table S1. Soil pH was analyzed by a glass electrode (PHS-3BW, Bante Instruments) with soil/water ratio of 1/2.5 (m/v). SOC and TN contents were quantified using an elemental analyzer (Vario MACRO cube, Elementar). HCl pretreatment was unnecessary as carbonate C is absent in these acidic soils. According to Lu (2000), HN was measured via the alkaline hydrolysis diffusion method with a soil/solution (NaOH, 1 M) of 1/5 (m/v). The molybdate colorimetric method with Na_2CO_3 fusion and NH_4F- HCl extraction (1/10, m/v) was used to measure TP and AP, respectively. TK and AK were analyzed following NaOH fusion and NH_4OAc extraction (1/10, w/v), respectively, with quantification by flame photometry. Soil CEC was measured using the ammonium acetate method (Lu, 2000). Ammonium acetate solution (1 M, pH 7.0) was used to saturate soil samples at a soil/solution ratio of 1/60 (m/v), and the process was repeated 3 to 5 times until no Ca^{2+} was detected in the suspension. Soil clay content (<0.002 mm) was measured by a laser diffraction particle size analyzer (Mastersizer 2000, Malvern Instruments Ltd.) with sodium hexametaphosphate dispersing solution (soil/solution of 1/12.5, m/v), suggested by Miller and Schaetzl (2011).

2.5. Statistical analysis

The data were expressed as mean ± standard deviation (SD). Shapiro-Wilk test and Levene's test were used to evaluate the normality and homogeneity of variances, respectively, for all the data; and data were ln-transformed when necessary. The significant difference of soil physicochemical and microbial properties among different sampling sites was analyzed with one-way ANOVA followed by Tukey's HSD test at a 0.05 probability level. The relationships among heavy metal variables, soil properties, and microbial features were explored using scatterplots and linear regression analyses, with the coefficient of determination (R^2) quantifying the strength of linear relationships. These statistical analyses were carried out by SPSS software (version 20.0, SPSS Inc.). Variation partitioning analysis (VPA) was performed with the functions "varpart" and "rda" in R 4.3.3 to quantify the respective contributions of heavy metal pollution (nemerow index), edaphic factors (soil pH, TN, TP, TK, HN, AP, AK, CEC, and clay), and microbial factors (MBC, amino sugars, microbial CUE, and microbial turnover time) to SOC variation. The random forest model (RF) was used to identify the main predictors of SOC among different variables, implemented with the "randomForest" package. The relative importance of each predictor was evaluated using the "rfPermute" package. The structure equation model (SEM) was established to assess the direct and indirect effects of heavy metal pollution, soil N availability, and microbial features on SOC, using AMOS (version 20.0, IBM AMOS). During SEM analysis, a prior model was constructed based on theoretical frameworks (Fig. S1), and then data were applied to the model. The final SEM was obtained through iterative refinement, whereby non-significant paths were systematically removed until all retained paths achieved statistical significance. The method of maximum-likelihood estimation was used for model fitting. The following parameters were evaluated as

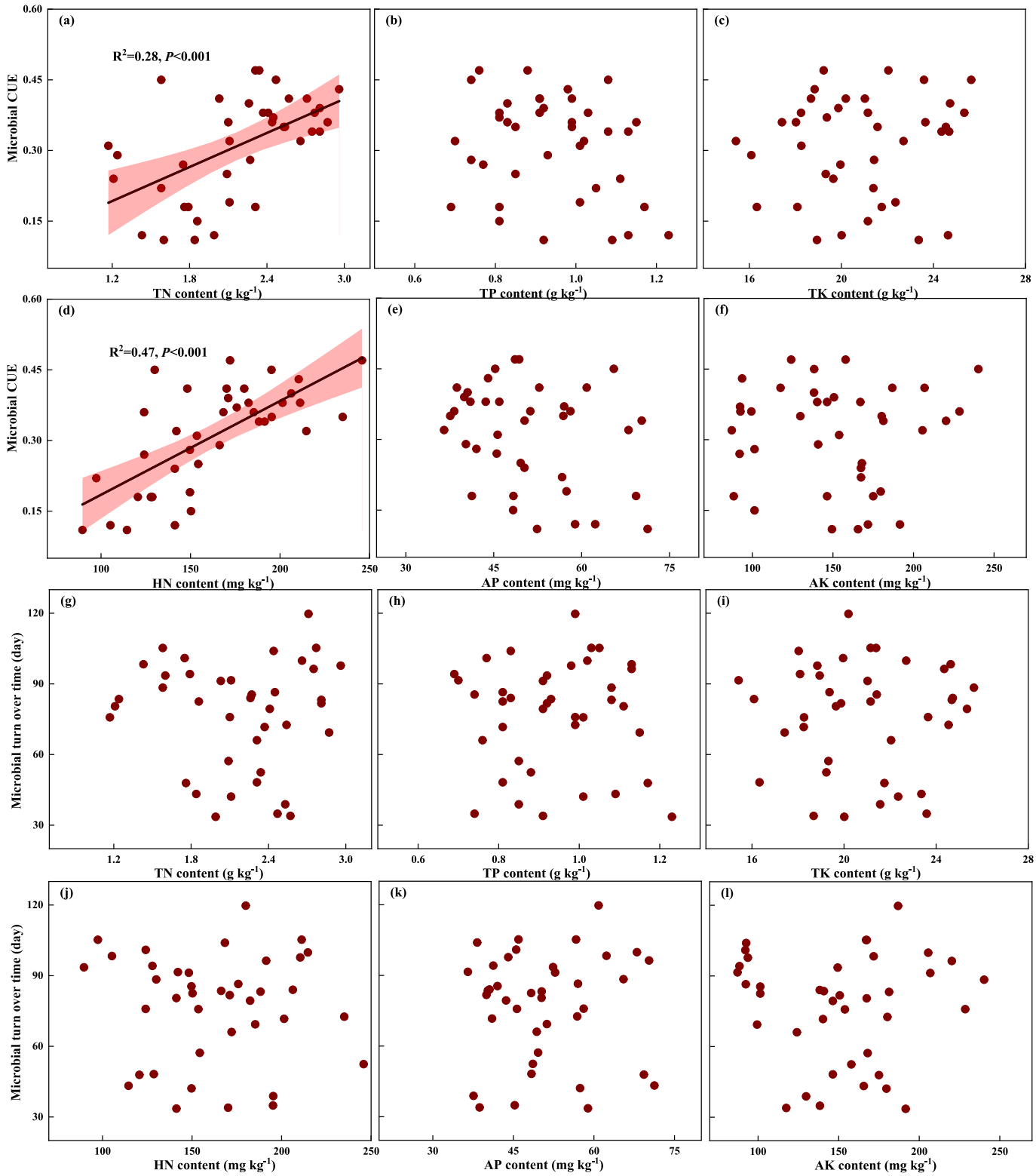

Fig. 5. Soil nutrients in relation to microbial physiological traits. (a-f) microbial CUE versus: (a) TN content, (b) TP content, (c) TK content, (d) HN content, (e) AP content, (f) AK content; (g-l) microbial turnover time versus: (g) TN content, (h) TP content, (i) TK content, (j) HN content, (k) AP content, (l) AK content.

model fit statistics: χ^2 statistic ($P > 0.05$), degrees of freedom (*df*), R^2 (explained proportion of variance), goodness-of-fit index (GFI > 0.90), root mean square error of approximation (RMSEA < 0.05), and akaike information criterion (AIC). All figures were depicted by Origin software (OriginPro 2022, OriginLab Corp.).

3. Results

3.1. Heavy metal contamination in the different sampling sites

According to the soil environmental quality standard for agricultural land in China (GB 15618–2018), the main heavy metal contaminants

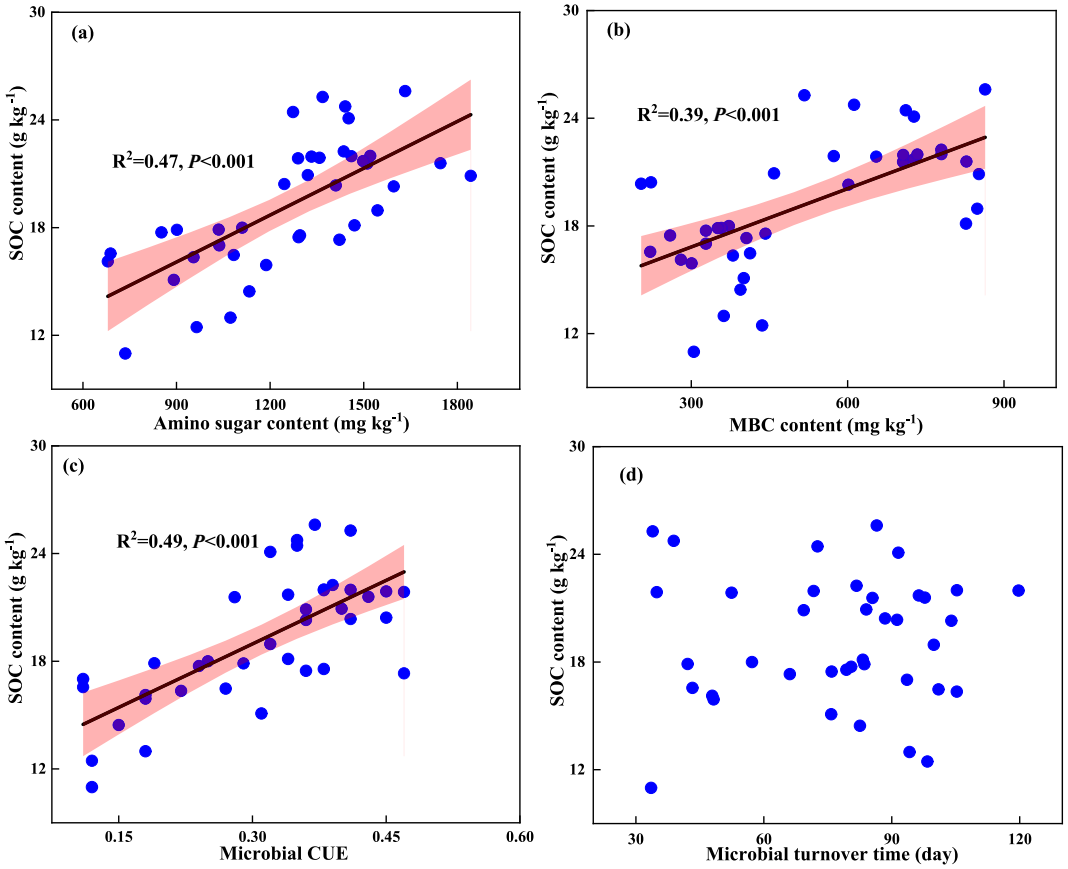

Fig. 6. Relationship between microbial variables and SOC content: (a) amino sugar content, (b) MBC content, (c) microbial CUE, (d) microbial turnover time.

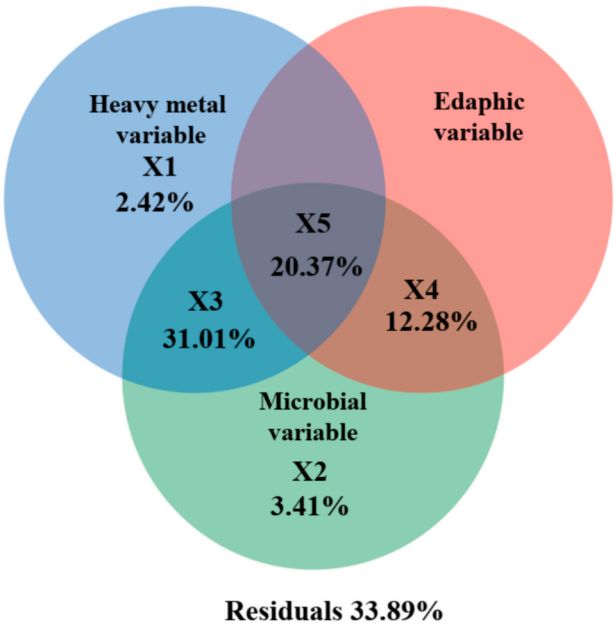

Fig. 7. Variation partitioning analysis of SOC variation. X1, fraction explained solely by heavy metals; X2, fraction explained solely by microbial factors; X3, fraction jointly explained by heavy metals and microbial factors; X4, fraction jointly explained by heavy metals and edaphic factors; X5, fraction jointly explained by the three groups of factors.

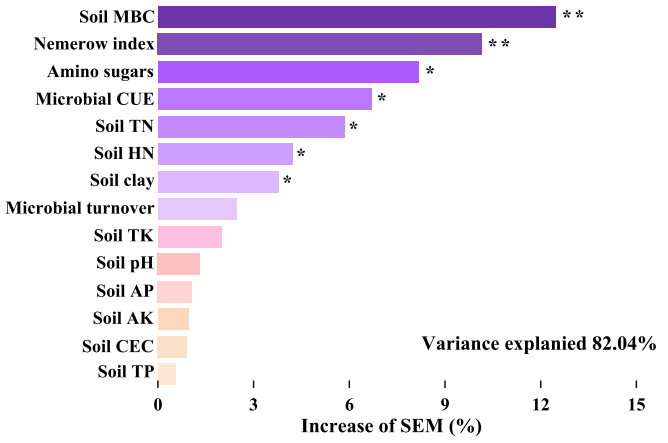

Fig. 8. Random forest analysis with permutation importance (% increase in MSE) of predictors for SOC variation. Significance level of each predictor is set as follows: * indicate $P < 0.05$; ** indicate $P < 0.01$.

were Cd and Cu (Table 1), while other metals (Hg, As, Pb, Cr, Ni, Zn) remained within screening values (Table S2). Soil Cd content ranged from 0.17 to 1.20 mg kg^{-1} across sampling sites, and Cu content varied between 29.68 and 193.33 mg kg^{-1}. Cd and Cu contents in all the sites exceeded the risk screening values (0.3 mg kg^{-1} for Cd and 50 mg kg^{-1} for Cu) according to GB 15618–2018, except S1 (Table 1), which was farthest from the mine (Fig. 1). The nemerow index ranged from 0.48 (S1) to 2.93 (S11) in our study.

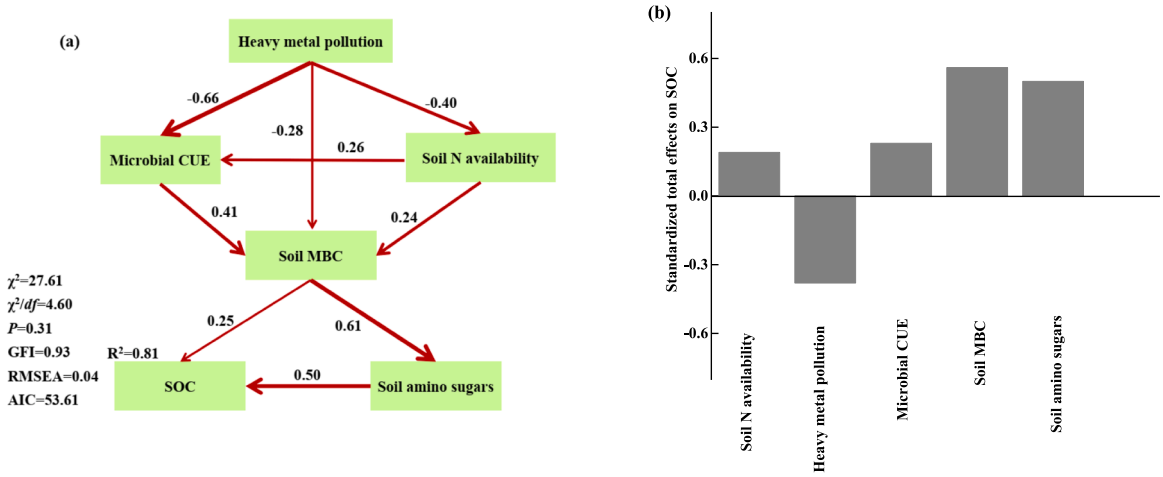

Fig. 9. (a) Structural equation model (SEM) depicting the effects of heavy metal pollution, microbial properties and soil N availability on SOC variation. The number adjacent to the arrow represents standardized path coefficient and the arrow width indicates the strength of the causal relationship. R^2 indicates the proportion of SOC variation explained by the SEM, and only significant paths ($P < 0.05$) are shown. (b) Standardized total effects (direct and indirect) of each variable on SOC derived from SEM.

3.2. Soil physicochemical and microbial properties in the different sampling sites

Soil pH across sampling sites exhibited typical acidity for cropland soils, with the highest value of 5.86 (S4). SOC content was highest at S6 (23.97 g kg^{-1}), significantly exceeding values at S9-S13, while the lowest level (14.56 g kg^{-1}) occurred at S13 (Table 2). TN content ranged from 1.21 to 2.80 g kg^{-1}, with S12 showing the lowest value (significantly lower than all sites except S9). TP content varied from 0.76 to 1.16 g kg^{-1}, and TK content showed minimal variation (18.00 to 24.03 g kg^{-1}) across sites. HN content was highest at S5 (227.41 mg kg^{-1}), while the lowest level (97.44 mg kg^{-1}) occurred at S9. AP and AK contents fluctuated between 38.94 and 66.47 mg kg^{-1} and 93.73 and 225.21mg kg^{-1}, respectively. Soil CEC ranged from 6.10 $cmol_{(+)}$ kg^{-1} (S1) to 13.28 $cmol_{(+)}$ kg^{-1} (S6). Clay content ranged from 11.75 % (S13) to 20.02 % (S3) (Table 2), showing a decreasing trend from upstream to downstream of the river (Fig. S2).

As to amino sugars, the greatest content of 1740.34 mg kg^{-1} was observed at S2, which was significantly higher than other sites, and the lowest content of 701.48 mg kg^{-1} occurred at S13 (Table 3). MBC content ranged from 228.55 mg kg^{-1} (S7) to 847.70 mg kg^{-1} (S2). Microbial CUE varied between 0.14 (S13) and 0.42 (S8), and microbial turnover time ranged from 35.90 days (S6) to 105.30 days (S4) (Table 3).

3.3. Relationship among heavy metal pollution, microbial features, and soil properties

Significant negative correlations were observed between nemerow index and microbial features, including amino sugars (Fig. 2a, R2 = 0.72, $P < 0.001$), MBC (Fig. 2b, R2 = 0.46, $P < 0.001$), microbial CUE (Fig. 2c, R2 = 0.42, $P < 0.001$), and microbial turnover time (Fig. 2d, R2 = 0.12, $P = 0.017$). For specific heavy metals, similar relationships were detected between soil Cd and Cu contents and microbial features (Fig. S3).

Nemerow index showed significant negative relationships with SOC (Fig. 3a; $R^2 = 0.46$, $P < 0.001$) and proportion of amino sugars to SOC (Fig. 3b; $R^2 = 0.13$, $P = 0.015$). Regarding soil nutrients, the index was negatively correlated with soil TN (Fig. 4a; $R^2 = 0.39$, $P < 0.001$) and HN (Fig. 4d; $R^2 = 0.19$, $P = 0.003$), but showed no correlation with TP (Fig. 4b), TK (Fig. 4c), AP (Fig. 4e), or AK (Fig. 4f). Soil Cd and Cu contents exhibited similar correlation patterns with SOC, proportion of amino sugars to SOC (Fig. S4), and soil nutrients (Fig. S5). These heavy metal variables correlated with clay content, but not with soil pH or CEC (Fig. S6).

Among soil nutrients, only soil TN and HN showed significant positive correlations with microbial CUE (Fig. 5a, d). In contrast, no nutrient variables correlated significantly with microbial turnover time (Fig. 5g-l). Moreover, microbial features were positively correlated with SOC content, including amino sugars (Fig. 6a, R2 = 0.47, $P < 0.001$), MBC (Fig. 6b, R2 = 0.39, $P < 0.001$), and microbial CUE (Fig. 6c, R2 = 0.49, $P < 0.001$). Contrary, no significant correlation was found between microbial turnover time and SOC (Fig. 6d).

3.4. Drivers of SOC variation under heavy metal contamination

The VPA result revealed that 69.49 % of SOC variation was collectively explained by heavy metals, edaphic properties, and microbial factors (Fig. 7). The largest contributor was the interaction between heavy metals and microbial factors (31.01 %), followed by the joint effect of three types of factors (20.37 %). Microbial factors independently accounted for 3.41 % of SOC variation, while heavy metals contributed 2.42 %. No unique effect of edaphic properties was detected.

The RF analysis explained 82.04 % of SOC variation with the selected variables (Fig. 8). Soil MBC and nemerow index were the two most important predictors, with amino sugars, microbial CUE, soil TN, HN, and soil clay also showing significant effects. According to RF result, SEM was constructed to quantify direct and indirect pathways influencing SOC. SEM explained 81 % of SOC variation with a good fitness indicating by χ^2/df, GFI, RMSEA, and AIC (Fig. 9a). Specifically, amino sugars (path coefficient = 0.50) and soil MBC (path coefficient = 0.25) showed direct and positive effects on SOC. Heavy metal pollution indirectly reduced SOC by suppressing MBC and amino sugars through impairing microbial CUE and soil N availability. Additionally, heavy metal pollution negatively influenced SOC by directly suppressing MBC (Fig. 9a). Consistent with RF analysis, MBC exhibited the strongest total effects (0.56) on SOC. Meanwhile, amino sugars (total effects = 0.50), heavy metal pollution (total effects = -0.38), microbial CUE (total effects = 0.23), and soil N availability (total effects = 0.19) could also be significant drivers of SOC variation (Fig. 9b).

4. Discussion

4.1. Response of microbial physiological traits to heavy metal contamination

Microbial CUE represents the balance of catabolic and anabolic activities that primarily determines SOC fate (Schimel and Schaeffer, 2012; Tao et al., 2023). The CUE values in our study ranged from 0.14 to 0.42 (Table 3), falling within the reported range in paddy soils using the ^{18}O-H_2O incubation method (Chen et al., 2020; Duan et al., 2024). Our first hypothesis that heavy metal contamination decreased microbial CUE and accelerated microbial biomass turnover was confirmed, as nemerow index exhibited negative correlations with microbial CUE (Fig. 2c) and biomass turnover time (Fig. 2d). Heavy metal pollution could impede normal electron and matter transport since heavy metal ions would accumulate in microbial intracellular region and cytoderm mainly through adsorption (Jin et al., 2018; Sarret et al., 1998). To alleviate this heavy metal stress, microorganisms would consume more substrates to produce energy and synthesize extracellular electron transport compounds, bypassing the inhibited intracellular electron transport chains (Bore et al., 2017). Consequently, microbes would change their C utilization strategy by preferentially allocating more resources to cellular repair and maintenance rather than growth and proliferation under this stress (Fließbach et al., 1994; Tripathy et al., 2014). Subsequently, the decreased microbial CUE in heavy metal-contaminated paddy soils was observed in our study (Fig. 2c). The reported increase in microbial metabolic quotient (qCO_2, defined as soil microbial respiration rate per unit of microbial biomass), also meant more energy is required for microbial maintenance under heavy metal pollution (Niemeyer et al., 2012; Zeng et al., 2024b). This phenomenon provided complementary evidence for our findings.

Altered diversity and composition of microbial community could also be a vital reason for reduced microbial CUE (Geyer et al., 2016). Enhanced microbial diversity broadens metabolic functional breadth, favoring efficient utilization of diverse C substrates that promote microbial growth, leading to a positive relationship between microbial diversity and CUE (Domeignoz-Horta et al., 2020; Yang et al., 2024). Previous studies confirmed that heavy metal stress diminished microbial diversity by inhibiting or eliminating metal-sensitive taxa due to cellular functions disruption and cell membrane and DNA structure damage (Abdu et al., 2017; Yin et al., 2023). Guo et al. (2022, 2023) documented a comparable heavy metal pollution dynamics in this region and demonstrated that heavy metal pollution decreased bacterial diversity but increased fungal diversity. This divergence was probably due to the fact that fungi possess a greater heavy metal tolerance than bacteria (Cooke and Whipps, 1993; Jiang et al., 2023). Moreover, bacterial community exhibit a higher CUE than fungal community, given the high cost of fungi in resource acquisition (Soares and Rousk, 2019), the observed CUE reduction in our study could be attributed to the decreased bacterial diversity under heavy metal contamination.

Moreover, soil nutrient availability critically influences microbial CUE (Liu et al., 2025; Manzoni et al., 2012), and positive relationships between the contents of soil TN and HN and the microbial CUE were also identified in our research (Fig. 5a, d). However, TN and HN were negatively correlated with nemerow index (Fig. 4a, d), suggesting that heavy metal pollution led to soil N deficiency. Given the essential role of biological N fixation in N cycling of paddy fields (Yang et al., 2022), this deficiency could be attributed to reduced diversity and richness of N-fixing bacteria under heavy metal stress (Wang et al., 2019). Furthermore, heavy metal pollution could increase soil N loss risk by stimulating microbial nitrification, denitrification, and dissimilatory nitrate reduction, as demonstrated in our study area by Guo et al. (2024). To cope with decreased N availability, microorganisms would invest more energy to extracellular enzyme production for N acquisition through accelerating soil organic matter decomposition (Manzoni et al., 2012). This energy reallocation ultimately decreased microbial CUE (Fig. 2c). Therefore, decreased soil N availability could be considered as another mechanism underlying the reduced microbial CUE with heavy metal contamination.

The microbial turnover time ranged from 35.90 days to 105.30 days (Table 3), consistent with the previously reported values (Cheng, 2009). The accelerated turnover of microbial biomass under heavy metal contamination (Fig. 2d) could be inferred from an increased cell death rates induced by the heavy metal cytotoxicity (Abdu et al., 2017). Nevertheless, the precise mechanisms require further elucidation due to limited mechanistic studies.

4.2. Implication of heavy metal contamination on SOC mediated by microbial anabolism in paddy soils

Plant C input is the primary origin of SOC, although our study did not collect direct plant biomass data, the absence of correlations between heavy metal variables and grain yield in the investigated fields indicated that plant biomass input was not significantly affected by heavy metal pollution in this study (Fig. S7). Previous studies suggested that heavy metal contamination decreased plant biomass in natural ecosystem (Hermle et al., 2006; Malunguja et al., 2022), contrasting with our results. This divergence could be attributed to suitable farmland management, such as appropriate fertilizer application, which mitigated the heavy metal phytotoxicity and maintained the crop productivity compared with natural ecosystem (Smith, 2009). Moreover, previous studies suggested that SOC content does not always correlate directly with C input quantity in agricultural soils, as microorganisms predominantly govern the fate of SOC (Kallenbach et al., 2015; Sokol and Bradford, 2018). The VPA and RF analyses revealed that microbial properties and heavy metal pollution jointly drove SOC variation, with microbial factors playing a dominant role. Notably, heavy metal pollution exerted a greater influence on SOC than native soil properties (Figs. 7, 8). SEM analysis indicated that heavy metal pollution could reduce SOC by decreasing MBC and microbial residues via negative effects on microbial CUE and soil N availability (Fig. 9a). The observed decrease in microbial CUE suggests a lower partitioning of C toward microbial growth during metabolic processes (Tao et al., 2023). Therefore, as by-products of microbial anabolism, microbial biomass formation and microbial residue accumulation were reduced under heavy metal contamination (Fig. 2a, b). Consequently, the decreased SOC (Fig. 3a) and proportion of amino sugars to SOC (Fig. 3b) were found under this context. These results strongly demonstrated that heavy metal pollution significantly decreased the accumulation of microbial residues by impairing microbial anabolic activities, ultimately compromising SOC storage. These findings therefore supported our second hypothesis that the attenuated microbial anabolism primarily drove SOC variation in heavy metal-polluted paddy soils.

On the other hand, previous studies proposed that acceleration of microbial biomass turnover could increase the production rate of microbial residues, potentially enhancing SOC accrual under environmental stressors such as warming (Hagerty et al. 2014; Wang et al., 2022). Although accelerated microbial biomass turnover was observed under heavy metal contamination in our study (Fig. 2d), it neither correlated with amino sugar content (Fig. S8) nor with SOC content (Fig. 6d). These results appeared contrary to the above publications. In fact, rapid microbial biomass turnover is expected to promote microbial residue production only under the necessary condition of stable or increased microbial growth rates (Hagerty et al. 2014; Prommer et al., 2019). Therefore, it was not surprising that no correlation was observed between microbial biomass turnover and amino sugars or SOC (Fig. 6d, S8), given that decreased microbial growth rate was measured under heavy metal pollution (Fig. S9).

5. Conclusions

A field investigation of heavy metal contamination in paddy soils was

conducted around an abandoned tungsten mining site. Heavy metal pollution was negatively correlated with microbial CUE and microbial biomass turnover, indicating significant alteration of microbial physiological traits in polluted paddy soils. The decrease of microbial CUE - suggested an impairment of microbial anabolism, meaning that a smaller proportion of C was allocated to microbial growth relative to respiration under heavy metal stress. Consequently, the C flow through the chain of "microbial substrates-microbial biomass-microbial residues" was diminished. This led to adverse effects of heavy metal pollution on MBC formation and microbial residue production, ultimately decreasing SOC storage. Although accelerated microbial biomass turnover was observed, it showed no correlation with amino sugars or SOC. This lack of correlation was attributed to the concurrent decrease in microbial growth rate caused by heavy metal pollution. In conclusion, the empirical evidences firmly supported that heavy metal pollution contributed to SOC loss in paddy fields by suppressing microbial anabolism with the reduced accumulation of microbial residues. Our research triggered a warning that heavy metal pollution would pose a substantial threat to soil C sequestration capacity in paddy soils.

CRediT authorship contribution statement

Li Xiong: Writing – original draft, Investigation, Funding acquisition, Formal analysis, Conceptualization. **Marios Drosos:** Writing – review & editing, Writing – original draft. **Min Jiao:** Investigation, Formal analysis. **Jianfei Sun:** Visualization, Methodology. **Guilong Li:** Methodology, Investigation, Formal analysis. **Longxin He:** Investigation, Formal analysis. **Fan Li:** Formal analysis, Data curation. **Cheng Liu:** Visualization, Formal analysis. **Antonio Scopa:** Writing – review & editing. **Wenjian Xia:** Writing – review & editing, Supervision, Investigation, Funding acquisition, Conceptualization. **Caihong Shao:** Methodology, Formal analysis. **Zengbing Liu:** Visualization, Methodology.

Declaration of competing interest

The authors declare that they have no known competing financial interests or personal relationships that could have appeared to influence the work reported in this paper.

Acknowledgements

This study was supported by the Basic Research and Talent Training Project of Jiangxi Academy of Agricultural Sciences (JXSNKYJCRC202415), the Jiangxi Provincial Natural Science Foundation (20232BAB215012), the Basic Research and Talent Training Project of Jiangxi Academy of Agricultural Sciences (JXSNKYJCRC202343), and the National Natural Science Foundation of China (Grant no. 32060726).

Appendix A. Supplementary data

Supplementary data to this article can be found online at https://doi.org/10.1016/j.geoderma.2025.117486.

Data availability

Data will be made available on request.

References

Abdu, N., Abdullahi, A.A., Abdulkadir, A., 2017. Heavy metals and soil microbes. Environ. Chem. Lett. 15, 65–84.
Batjes, N.H., 1996. Total carbon and nitrogen in the soils of the world. Eur. J. Soil Sci. 47, 151–163.
Bian, R., Cheng, K., Zheng, J., Liu, X., Liu, Y., Li, Z., Li, L., Smith, P., Pan, G., Crowley, D., Zheng, J., Zhang, X., Zhang, L., Hussain, Q., 2015. Does metal pollution matter with C retention by rice soil? Sci. Rep. 5, 13233.
Bore, E.K., Apostel, C., Halicki, S., Kuzyakov, Y., Dippold, M.A., 2017. Soil microorganisms can overcome respiration inhibition by coupling intra-and extracellular metabolism: ^{13}C metabolic tracing.
Chen, X., Hu, Y., Xia, Y., Zheng, S., Ma, C., Rui, Y., He, H., Huang, D., Zhang, Z., Ge, T., Wu, J., Guggenberger, G., Kuzyakov, Y., Su, Y., 2021. Contrasting pathways of carbon sequestration in paddy and upland soils. Glob. Chang. Biol. 27, 2478–2490.
Chen, X., Xia, Y., Rui, Y., Ning, Z., Hu, Y., Tang, H., He, H., Li, H., Kuzyakov, Y., Ge, T., Wu, J., Su, Y., 2020. Microbial carbon use efficiency, biomass turnover, and necromass accumulation in paddy soil depending on fertilization. Agr. Ecosyst. Environ. 292, 106816.
Cheng, W., 2009. Rhizosphere priming effect: its functional relationships with microbial turnover, evapotranspiration, and C-N budgets. Soil Biol. Biochem. 41, 1795–1801.
Cooke, R.C., Whipps, J.M., 1993. Ecophysiology of fungi, first ed. Willey-Blackwell, Oxford.
Cotrufo, M.F., Wallenstein, M.D., Boot, C.M., Denef, K., Paul, E., 2013. The microbial efficiency-matrix stabilization (MEMS) framework integrates plant litter decomposition with soil organic matter? Glob. Chang. Biol. 19, 988–995.
Dai, J., Becquer, T., Rouiller, J.H., Reversat, G., Bernhard-Reversat, F., Lavelle, P., 2004. Influence of heavy metals on C and N mineralisation and microbial biomass in Zn-, Pb-, Cu-, and Cd-contaminated soils. Appl. Soil Ecol. 25, 99–109.
Domeignoz-Horta, L.A., Pold, G., Liu, X.J.A., Frey, S.D., Melillo, J.M., DeAngelis, K.M., 2020. Microbial diversity drives carbon use efficiency in a model soil. Nat. Commun. 11, 3684.
Duan, X., Rui, Y., Xia, Y., Hu, Y., Ma, C., Qiao, H., Zeng, G., Su, Y., Wu, J., Chen, X., 2024. Higher microbial C use efficiency in paddy than in adjacent upland soils: evidence from continental scale. Soil Tillage Res. 235, 105891.
Enya, O., Heaney, N., Iniama, G., Lin, C., 2020. Effects of heavy metals on organic matter decomposition in inundated soils: microcosm experiment and field examination. Sci. Total Environ. 724, 138223.
Fließbach, A., Martens, R., Reber, H.H., 1994. Soil microbial biomass and microbial activity in soils treated with heavy metal contaminated sewage sludge. Soil Biol. Biochem. 26, 1201–1205.
Georgiou, K., Abramoff, R.Z., Harte, J., Riley, W.J., Torn, M.S., 2017. Microbial community-level regulation explains soil carbon responses to long-term litter manipulations. Nat. Commun. 8, 1223.
Geyer, M.K., Kyker-snowman, E., Grandy, S.A., Frey, S.D., 2016. Microbial carbon use efficiency: accounting for population, community, and ecosystem-scale controls over the fate of metabolized organic matter. Biogeochemistry 127, 173–188.
Guo, Y., Cheng, S., Fang, H., Yang, Y., Li, Y., Zhou, Y., 2022. Responses of soil fungal taxonomic attributes and enzyme activities to copper and cadmium co-contamination in paddy soils. Sci. Total Environ. 844, 157119.
Guo, Y., Cheng, S., Fang, H., Yang, Y., Li, Y., Shi, F., Zhou, Y., 2023. Copper and cadmium co-contamination affects soil bacterial taxonomic and functional attributes in paddy soils. Environ. Pollut. 329, 121724.
Guo, Y., Cheng, S., Fang, H., Geng, J., Li, Y., Shi, F., Wang, H., Chen, L., Zhou, Y., 2024. Copper and cadmium co-contamination increases the risk of nitrogen loss in red paddy soils. J. Hazard. Mater. 479, 135626.
Hagerty, S.B., van Groenigen, K.J., Allison, S.D., Hungate, B.A., Schwartz, E., Koch, G.W., Kolka, R.K., Dijkstra, P., 2014. Accelerated microbial turnover but constant growth efficiency with warming in soil. Nat. Clim. Chang. 4, 903–906.
He, P., Zhang, Y., Shen, Q., Ling, N., Nan, Z., 2023. Microbial carbon use efficiency in different ecosystems: a meta-analysis based on a biogeochemical equilibrium model. Glob. Chang. Biol. 29, 4758–4774.
Hermle, S., Günthardt-Goerg, M.S., Schulin, R., 2006. Effects of metal-contaminated soil on the performance of young trees growing in model ecosystems under field conditions. Environ. Pollut. 144, 703–714.
Jiang, R., Wang, M., Chen, W., 2023. Heavy metal pollution triggers a shift from bacteria-based to fungi-based soil micro-food web: evidence from an abandoned mining-smelting area. J. Hazard. Mater. 459, 132164.
Jiang, Z., Guo, Z., Peng, C., Liu, X., Zhou, Z., Xiao, X., 2021. Heavy metals in soils around non-ferrous smelteries in China: status, health risks and control measures. Environ. Pollut. 282, 117038.
Jin, Y., Luan, Y., Ning, Y., Wang, L., 2018. Effects and mechanisms of microbial remediation of heavy metals in soil: a critical review. Appl. Sci. 8, 1336.
Jobbágy, E.G., Jackson, R.B., 2000. The vertical distribution of soil organic carbon and its relation to climate and vegetation. Ecol. Appl. 10, 423–436.
Kallenbach, C.M., Grandy, A.S., Frey, S.D., Diefendorf, A.F., 2015. Microbial physiology and residues regulate agricultural soil carbon accumulation. Soil Biol. Biochem. 91, 279–290.
Kandeler, E., Tscherko, D., Bruce, K.D., Stemmer, M., Hobbs, P.J., Bardgett, R.D., Amelung, W., 2000. Structure and function of the soil microbial community in microhabitats of a heavy metal polluted soil. Biol. Fertil. Soils 32, 390–400.
Khan, S., Naushad, M., Lima, E.C., Zhang, S., Shaheen, S.M., Rinklebe, J., 2021. Global soil pollution by toxic elements: current status and future perspectives on the risk assessment and remediation strategies-a review. J. Hazard. Mater. 471, 126039.
Lal, R., 2004. Soil carbon sequestration impacts on global climate change and food security. Science 304, 1623–1627.
Liang, C., Schimel, J.P., Jastrow, J.D., 2017. The importance of anabolism in microbial control over soil carbon storage. Nat. Microbiol. 2, 1–6.
Liu, M., Lin, H., Li, J., 2025. Are there links between nutrient inputs and the response of microbial carbon use efficiency or soil organic carbon? A Meta-Analysis. Soil Biol. Biochem. 201, 109656.

Lin, Y., Ye, Y., Hu, Y., Shi, H., 2019. The variation in microbial community structure under different heavy metal contamination levels in paddy soils. Ecotoxicol. Environ. Saf. 180, 557–564.
Liu, X., Xu, X., Ma, T., Zhou, S., Bi, X., He, H., Zhang, X., Li, W., 2023. Linking microbial carbon pump capacity and efficacy to soil organic carbon storage and stability under heavy metal pollution. Soil Ecol. Lett. 5, 220140.
Liu, Y., Ge, T., van Groenigen, K.J., Yang, Y., Wang, P., Cheng, K., Zhu, Z., Wang, J., Li, Y., Guggenberger, G., Sardans, J., Penuelas, J., Wu, J., Kuzyakov, Y., 2021. Rice paddy soils are a quantitatively important carbon store according to a global synthesis. Commun. Earth Environ. 2, 154.
Lu, R., 2000. Analytical methods for soil agricultural chemistry, first ed. China Agricultural Science and Technology Press, Beijing (in Chinese).
Malunguja, G.K., Thakur, B., Devi, A., 2022. Heavy metal contamination of forest soils by vehicular emissions: ecological risks and effects on tree productivity. Environ. Process. 9, 11.
Manzoni, S., Taylor, P., Richter, A., Porporato, A., Ågren, G.I., 2012. Environmental and stoichiometric controls on microbial carbon use efficiency in soils. New Phytol. 196, 79–91.
Miller, B.A., Schaetzl, R.J., 2011. Precision of soil particle size analysis using laser diffractometry. Soil Sci. Soc. Am. J. 76, 1719–1727.
Niemeyer, J.C., Lolata, G.B., Carvalho, G.M.D., Da Silva, E.M., Sousa, J.P., Nogueira, M. A., 2012. Microbial indicators of soil health as tools for ecological risk assessment of a metal contaminated site in Brazil. Appl. Soil Ecol. 59, 96–105.
Ohm, H., Marschner, B., Broos, K., 2011. Respiration and priming effects after fructose and alanine additions in two copper- and zinc-contaminated Australian soils. Biol. Fertil. Soils 47, 523–532.
Paterson, E., Midwood, A.J., Millard, P., 2009. Through the eye of the needle: a review of isotope approaches to quantify microbial processes mediating soil carbon balance. New Phytol. 184, 19–33.
Prommer, J., Walker, T.W.N., Wanek, W., Braun, J., Zezula, D., Hu, Y., Hofhansl, F., Richter, A., 2019. Increased microbial growth, biomass, and turnover drive soil organic carbon accumulation at higher plant diversity. Glob. Chang. Biol. 26, 669–681.
Qin, G., Niu, Z., Yu, J., Li, Z., Ma, J., Xiang, P., 2021. Soil heavy metal pollution and food safety in China: effects, sources and removing technology. Chemosphere 267, 129205.
Sarret, G., Manceau, A., Spadini, L., Roux, J.C., Hazemann, J.L., Soldo, Y., Eybert-Bérard, L., Menthonnex, J., 1998. Structural determination of Zn and Pb binding sites in *Penicillium chrysogenum* cell walls by EXAFS spectroscopy. Environ. Sci. Technol. 32, 1648–1655.
Schimel, J.P., Schaeffer, S.M., 2012. Microbial control over carbon cycling in soil. Front. Microbiol. 3, 348.
Smith, S.R., 2009. A critical review of the bioavailability and impacts of heavy metals in municipal solid waste composts compared to sewage sludge. Environ. Int. 35, 142–156.
Soares, M., Rousk, J., 2019. Microbial growth and carbon use efficiency in soil: links to fungal-bacterial dominance. SOC-Quality and Stoichiometry. Soil Biol. Biochem. 131, 195–205.
Sokol, N.W., Bradford, M.A., 2018. Microbial formation of stable soil carbon is more efficient from belowground than aboveground input. Nat. Geosci. 12, 46–53.
Spohn, M., Klaus, K., Wanek, W., Richter, A., 2016. Microbial carbon use efficiency and biomass turnover times depending on soil depth-implications for carbon cycling. Soil Biol. Biochem. 96, 74–81.
Tao, F., Huang, Y., Hungate, B.A., Manzoni, S., Frey, S.D., Schmidt, M.W.I., Reichstein, M., Carvalhais, N., Ciais, P., Jiang, L., Lehmann, J., Wang, Y.P., Houlton, B.Z., Ahrens, B., Mishra, U., Hugelius, G., Hocking, T.D., Lu, X., Shi, Z., Viatkin, K., Vargas, R., Yigini, Y., Omuto, C., Malik, A.A., Peralta, G., Cuevas-Corona., R., Di Paolo, L.E., Luotto, I., Liao, C., Liang, Y.S., Saynes, V.S., Huang, X., Luo, Y., 2023. Microbial carbon use efficiency promotes global soil carbon storage. Nature 618, 981-985.
Tomczyk, P., Wdowczyk, A., Wiatkowska, B., Szymańska-Pulikowska, A., 2023. Assessment of heavy metal contamination of agricultural soils in Poland using contamination indicators. Ecol. Ind. 156, 111161.
Tripathy, S., Bhattacharyya, P., Mohapatra, R., Som, A., Chowdhury, D., 2014. Influence of different fractions of heavy metals on microbial ecophysiological indicators and enzyme activities in century old municipal solid waste amended soil. Ecol. Eng. 70, 25–34.
Wang, C., Qu, L., Yang, L., Liu, D., Morrissey, E., Miao, R., Liu, Z., Wang, Q., Fang, Y., Bai, E., 2021. Large-scale importance of microbial carbon use efficiency and residues to soil organic carbon. Glob. Chang. Biol. 27, 2039–2048.
Wang, C., Wu, B., Jiang, K., Wei, M., Wang, S., 2019. Effects of different concentrations and types of Cu and Pb on soil N-fixing bacterial communities in the wheat rhizosphere. Appl. Soil Ecol. 144, 51–59.
Wang, M., Dungait, J.A.J., Wei, X., Ge, T., Hou, R., Ouyang, Z., Zhang, F., Tian, J., 2022a. Long-term warming increased microbial carbon use efficiency and turnover rate under conservation tillage system. Soil Biol. Biochem. 172, 108770.
Wang, X., Cui, Y., Chen, L., Tang, K., Wang, D., Zhang, Z., Yu, J., Fang, L., 2022b. Microbial metabolic limitation and carbon use feedback in lead contaminated agricultural soils. Chemosphere 308, 136311.
Wei, L., Ge, T., Zhu, Z., Ye, R., Peñuelas, J., Li, Y., Lynn, T.M., Jones, D.L., Wu, J., Kuzyakov, Y., 2022. Paddy soils have a much higher microbial biomass content than upland soils: a review of the origin, mechanisms, and drivers. Agric. Ecosyst. Environ. 326, 107798.
Wu, J., Joergensen, R.G., Pommerening, B., Chaussod, R., Brookes, P.C., 1990. Measurement of soil microbial biomass C by fumigation-extraction-an automated procedure, Soil Biol. Biochem. 22, 1167–1169.
Xiao, K.Q., Zhao, Y., Liang, C., Zhao, M., Moore, O.W., Otero-Fariña, A., Zhu, Y.G., Johnson, K., Peacock, C.L., 2023a. Introducing the soil mineral carbon pump. Nat. Rev. Earth Environ. 4, 135–136.
Xiao, Z., Duan, C., Li, S., Chen, J., Peng, C., Che, R., Liu, C., Huang, Y., Mei, R., Xu, L., Lou, P., Yu, Y., 2023b. The microbial mechanisms by which long-term heavy metal contamination affects soil organic carbon levels. Chemosphere 340, 139770.
Xu, Y., Seshadri, B., Sarkar, B., Wang, H., Rumpel, C., Sparks, D., Farrell, M., Hall, T., Yang, X., Bolan, N., 2018. Biochar modulates heavy metal toxicity and improves microbial carbon use efficiency in soil. Sci. Total Environ. 621, 148–159.
Yang, Z., Chen, X., Hou, J., Liu, H., Tan, W., 2022. Soil texture and pH exhibit important effects on biological nitrogen fixation in paddy soil. Appl. Soil Ecol. 178, 104571.
Yang, Z., Zhu, Q., Zhang, Y., Jiang, P., Wang, Y., Fei, J., Rong, X., Peng, J., Wei, X., Luo, G., 2024. Soil carbon storage and accessibility drive microbial carbon use efficiency by regulating microbial diversity and key taxa in intercropping ecosystems. Biol. Fertil. Soils 60, 437–453.
Yin, Y., Wang, X., Hu, Y., Li, F., Cheng, H., 2023. Soil bacterial community structure in the habitats with different levels of heavy metal pollution at an abandoned polymetallic mine. J. Hazard. Mater. 442, 130063.
Zeng, K., Huang, X., Dai, C., He, C., Chen, H., Guo, J., Xin, G., 2024a. Bacterial community regulation of soil organic matter molecular structure in heavy metal-rich mangrove sediments. J. Hazard. Mater. 465, 133086.
Zeng, K., Huang, X., Guo, J., Dai, C., He, C., Chen, H., Xin, G., 2024b. Microbial-driven mechanisms for the effects of heavy metals on soil organic carbon storage: a global analysis. Environ. Int. 184, 108467.
Zhang, X., Amelung, W., 1996. Gas chromatographic determination of muramic acid, glucosamine, mannosamine, and galactosamine in soils. Soil Biol. Biochem. 28, 1201–1206.